J Therm Anal Calorim (2011) 105:845–849
DOI 10.1007/s10973-011-1701-8

Isothermal crystallization of P3HT:PCBM blends studied by RHC

Fatma Demir · Niko Van den Brande · Bruno Van Mele · Sabine Bertho · Dirk Vanderzande · Jean Manca · Guy Van Assche

ESTAC2010 Conference Special Issue

Abstract Defining appropriate annealing temperatures and times is vitally important for increasing the efficiency of bulk heterojunction solar cells by favoring the crystallinity of the polymer-fullerene blend components. In order to better understand the annealing process, the isothermal crystallization of poly(3-hexyl thiophene) (P3HT) and [6,6]-phenyl C_{61}-butyric acid methyl ester (PCBM) blend investigated by means of rapid heating cooling calorimetry (RHC). Isothermal crystallization experiments at temperatures in between the glass transition and melting, within the temperature range of 70–150 °C, can successfully be performed since RHC permits cooling at a sufficiently high rate in order to prevent crystallization during cooling. Crystallization isotherms were determined from the subsequent melting behavior of the blend. They were measured for a wide set of annealing temperatures and times, and the evolution of the crystallization rate with temperature is compared for annealing from the glassy state and from the melt state.

Keywords Isothermal crystallization · P3HT:PCBM · Solar cells · Annealing · Fast-scanning calorimetry

F. Demir · N. Van den Brande · B. Van Mele · G. Van Assche (✉)
Department of Physical Chemistry and Polymer Science, Faculty of Engineering, Vrije Universiteit Brussel, Pleinlaan 2, 1050 Brussels, Belgium
e-mail: gvassche@vub.ac.be

S. Bertho · D. Vanderzande · J. Manca
Institute for Materials for Research, Hasselt University, Wetenschapspark 1, 3590 Diepenbeek, Belgium

Introduction

Solar cells made of P3HT:PCBM are the state of the art for polymer:fullerene solar cells since the blend can generate 3.5–5% efficiency after post production annealing [1]. Annealing treatments increase the efficiency of the as-produced bulk heterojunction solar cells by forming a well-ordered morphology that creates better transportation pathways for charges to flow toward the corresponding electrodes. It is generally accepted that thermal annealing increases the crystallinity of the components, leading to a nanoscale phase separation, and consequently increases the device efficiency [2–6]. For an optimal efficiency and performance of the solar cells, a finely dispersed phase morphology with crystalline P3HT and PCBM structures of 5–20 nm dimensions is thought to be required [3, 7, 8]. To attain this, the thermal annealing conditions need to be tuned carefully. Too high temperatures or too long annealing times can induce a decrease of the efficiency due to the overgrowth of the crystals [9, 10].

As the crystallization is dominating the morphology formation during annealing, and as defining suitable annealing temperatures and times is vitally important for highly efficient solar cells, the isothermal crystallization of a P3HT:PCBM 1:1 blend was investigated in this study.

In order to investigate the nucleation and growth of the crystals formed during the isothermal annealing, one needs to avoid nuclei formation and crystal growth processes on cooling. Since conventional DSC techniques cannot cool fast enough to prevent crystallization on cooling, the isothermal crystallization studies are done by rapid heating cooling calorimetry (RHC). RHC was previously used in studies of polymer crystallization, medicines, and nanocomposites [11–13]. Also other fast DSC techniques have been used for crystallization kinetic studies of polymers

[14–16]. RHC is a fast-scanning DSC technique developed by TA Instruments [17], having a ten times smaller furnace heated by Infrared light. The RHC permits to heat at rates of up to 2000 K min^{-1} using sample sizes of about 50–500 μg. Cooling rates of 750 and 500 K min^{-1} can be reached down to 60 and 0 °C, respectively, the rate being limited by the heat transfer to the liquid nitrogen cooling device.

In this study, the faster cooling and heating by RHC is exploited to give well-controlled thermal annealing treatments to P3HT:PCBM blends, to quench the blends to an amorphous state below their glass transition (for annealing from the glassy state), and to study the glass transition, the cold crystallization, and the melting of thermally annealed blends with high sensitivity.

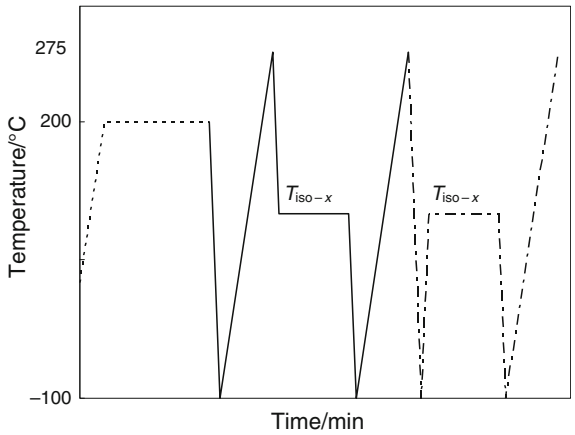

Fig. 1 Schematic representation of the typical sections of the temperature program: the melting and homogenization (*dashed*), the isothermal crystallization from the melt (*solid*), and the isothermal crystallization from the glassy state (*dot-dashed*)

Experimental

Mixtures with equal amounts (1:1 wt/wt) of P3HT (Merck, M_w = 35,000 g mol^{-1}, M_w/M_n = 1.8; regioregularity greater than 98.5%; T_m = 210 °C [18]) and PCBM (Solenne) were dissolved in chlorobenzene with a concentration of about 1 wt% and stirred overnight at 50 °C. The solution was deposited by drop-casting on large glass plates in the glove box under a nitrogen atmosphere to form films with a thickness of 1 μm. After drying in nitrogen atmosphere at room temperature for 50 h to remove the residual solvent, the remaining solid films were scratched off the glass substrates and collected as a powder for RHC measurements.

Rapid-scanning DSC experiments were performed on a prototype RHC of TA Instruments, equipped with a Liquid Nitrogen cooling and specifically designed for operation at high scanning rates. Tzero calibration was performed at 250 K min^{-1} with sapphire disks and the temperature and enthalpy calibration were performed using an indium standard. Experiments were conducted using Neon (6 mL min^{-1}) as a purge gas. Aluminum RHC crucibles weighing less than 2 mg were filled with sample masses in the range of 220–270 μg.

As a pre-treatment, the sample was kept for 10 min at 200 °C to melt it completely and to insure that it is homogeneous (the melting peak in a 1:1 P3HT:PCBM blend is at about 190 °C [18]). The pre-treatment temperature is a carefully chosen compromise between melting the crystals, homogenizing the blend, and avoiding degradation. Afterwards, the sample is rapidly cooled either to the desired crystallization temperatures (T_{iso-x}) for the crystallization from the melt state, or cooled down to −100 °C first and then heated up to T_{iso-x} for the isothermal crystallization from the glassy state (Fig. 1). The samples were cooled ballistically to avoid crystallization during the cooling. Samples were isothermally crystallized at different temperatures, both from the glassy state and from the melt state for a wide range of isothermal times. By subsequent heating (at 250 K min^{-1}) through its melting transition, the created crystals were molten and the melting peak is detected. The sample is heated to above its melting temperature (to 275 °C) for 0.1 min to remove the crystals and to erase the thermal history. An example of the temperature program is given in Fig. 1. Measurements for annealing from the glassy state and melt state were performed on fresh samples.

Results and discussion

For this study, it is vital to control the heating and cooling rate in the temperature range of importance. The plot of the derivative (sample sensor) temperature versus temperature for heating rates of 250 and 500 K min^{-1} and for ballistic cooling is shown in Fig. 2. It is clear that the heating rate is stable in the temperature range from −50 to 250 °C.

The samples were cooled ballistically: a non-controlled cooling rate of more than 1500 K min^{-1} is reached in the beginning and cooling was faster than 750 K min^{-1} down to 60 °C (just above the T_g of the blend). As equal amounts of cold crystallization and melting are obtained in the heating following a ballistic cooling to −100 °C, the cooling rate reached is sufficiently fast to avoid crystallization during cooling.

As the heat effect during the isothermal annealing is in general too small to be detected, the progress of the isothermal crystallization is evaluated through the melting in the subsequent heating. The melting peak can be preceded by a cold crystallization peak (Fig. 3).

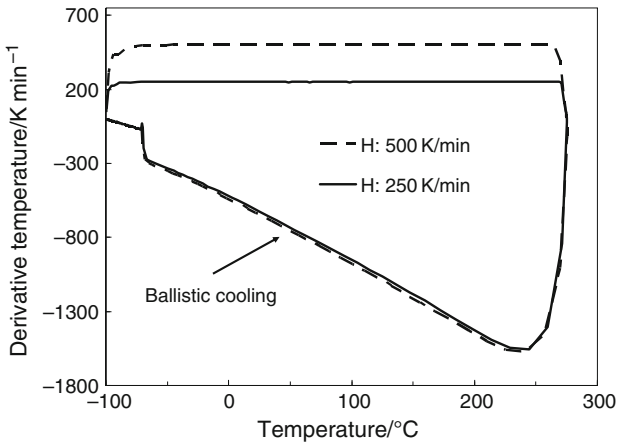

Fig. 2 Derivative temperature versus temperature plots for heating at 250 and 500 K min^{-1} and for the non-controlled (ballistic) cooling

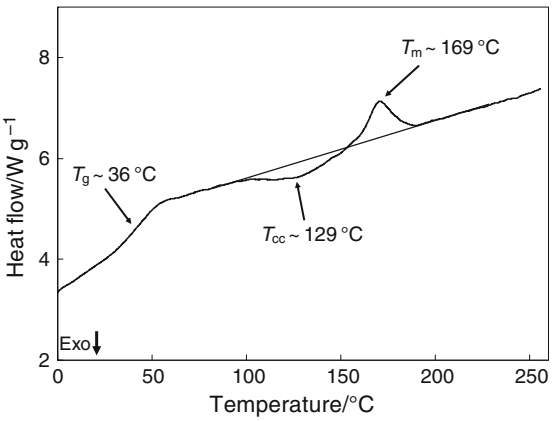

Fig. 3 RHC curve for the thermal transitions of a P3HT: PCBM 1:1 blend after quenching in the RHC, showing the glass transition T_g, cold crystallization T_{cc}, and melting T_m

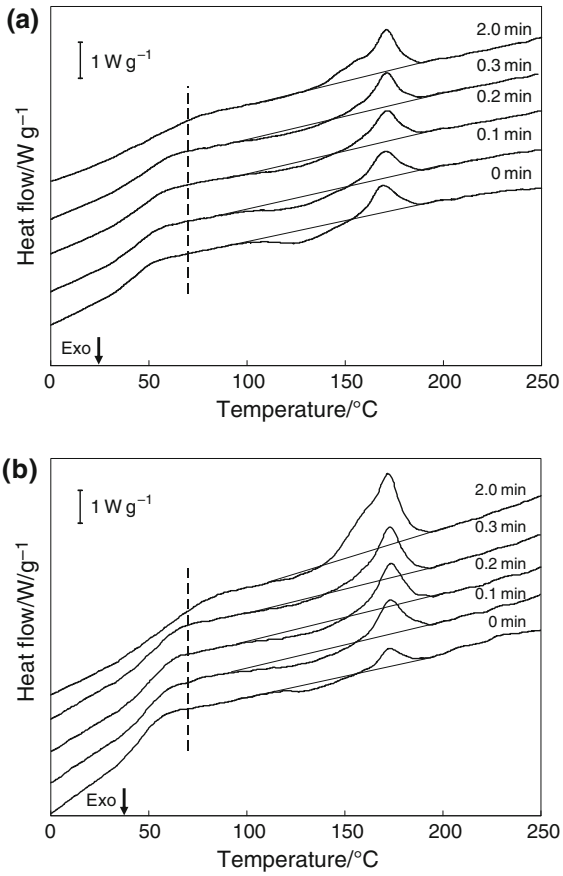

Fig. 4 RHC curves showing the heating of P3HT:PCBM 1:1 blend **a** at 250 K min^{-1} and **b** at 500 K min^{-1} after annealing at 125 °C from the glassy states for different times (as indicated). All curves are shifted vertically for clarity. The *vertical dashed line* indicates 70 °C

It is noticed that the cold crystallization peak gradually decreases with longer annealing times, while the melting peak increases (Fig. 4a). In addition to the decrease in cold crystallization and the increase in melting, the step in T_g is getting smaller with longer annealing times. As more crystals are created during the annealing, less remaining amorphous fraction is detected upon heating. For higher annealing times, a shoulder develops about 20 °C below the main melting peak.

The heating curves at 500 K min^{-1} after isothermal annealing at the same temperature as in Fig. 4a (125 °C) are given in Fig. 4b. It is obvious that less cold crystallization is occurring at a higher heating rate and consequently a lower melting peak is observed (see curves at 0 min). At higher heating rates, the sample has less time to crystallize during the heating, therefore cold crystallization is reduced and a smaller melting peak is observed. For the experiments at 500 K min^{-1}, an increase in cold crystallization and melting is seen for 0.1 min of annealing (compared to without annealing). This indicates the increase of the number of active nuclei during the initial 0.1 min of annealing significantly affects the cold crystallization rate. At 250 K min^{-1} this is not observed. Probably too many nuclei are formed during the slower heating to see the effect of the nuclei formed during the first 0.1 min of isothermal annealing.

Since pure P3HT has a T_g around 0–25 °C and PCBM has a T_g around 130 °C [18], the crystallization of P3HT from the blend, enriching the fraction of PCBM in the amorphous phase, leads to a higher T_g in the subsequent heating. This can be seen by comparing the T_g with the dashed line at 70 °C (Fig. 4a, b). An additional contribution of the formation of a rigid amorphous phase resulting from the finely dispersed crystalline structures can not be excluded.

The difference between the areas of the melting and the cold crystallization peaks, obtained by integration between limits before cold crystallization and after melting (see integration baselines in Fig. 4a, b), provides the heat evolved during the isothermal crystallization process

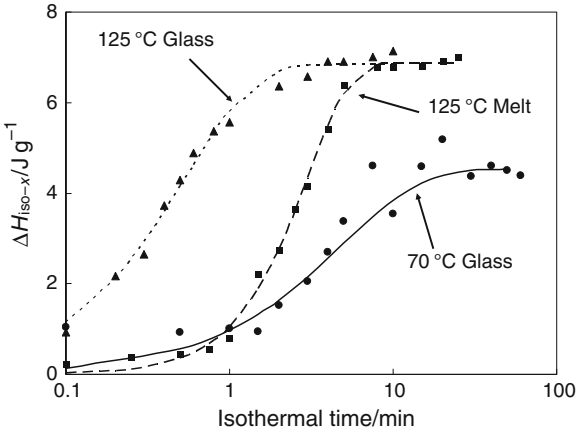

Fig. 5 Isothermal crystallization enthalpy versus annealing time showing experimental data (*symbols*) and Avrami model plots (*lines*) for annealing at 70 °C from the glassy state and at 125 °C from both the glassy and melt states

(ΔH_{iso-x}). ΔH_{iso-x} versus time plots are shown in Fig. 5, displaying sigmoidal curves for blends annealed at 70 °C after heating from the glassy amorphous state and for blends annealed at 125 °C after heating from the glassy state and after cooling from the melt state. The curves were fitted by the Avrami kinetics model [19], which is used to describe the evolution of the relative fraction of crystals as a function of time:

$$\chi = 1 - \exp(-kt^n)$$

where χ is the relative crystallinity during the isothermal crystallization at time t, n is the Avrami exponent, k is a function of temperature. The relative crystallinity $\chi(t)$ was calculated by dividing $\Delta H_{iso-x}(t)$ by the final ΔH_{iso-x} value reached for that experiment. The final ΔH_{iso-x} values for annealing from the glassy state and the melt state at 125 °C are equal; indicating the final blend crystallinity is similar even though the evolution of the crystallization differs. The curve for annealing at 70 °C from the glassy state has a smaller final ΔH_{iso-x} value, probably because at lower temperatures the blend is closer to its glass transition temperature and less mobility is available to crystallize. As mentioned earlier, the T_g of the remaining amorphous phase (enriched in PCBM) increases as P3HT crystallizes. At 70 °C, this will lead to a crystallization-induced vitrification when the composition reaches approximately 60 wt% of PCBM, as deduced from T_g-composition data published in [18]. For the curves corresponding to 2 min annealing at 125 °C in Fig. 4a, b, the dashed line of 70 °C is indeed within the glass transition region. At 150 °C the final ΔH_{iso-x} value is also smaller than that of 125 °C (see Table 1), which can be attributed to the fact that this temperature is within the start of the melting endotherm, preventing the crystallization of less perfect crystals.

Table 1 The time at half crystallization ($t_{½}$), crystallization rate ($1/t_{½}$), and final enthalpy of crystallization for isothermal annealing experiments in different conditions

β/K/min	T_{iso-x}/°C	Annealing from	$t_{½}$/min	$1/t_{½}$/min^{-1}	Final ΔH_{iso-x}/J/g
250	70	Glass	3.3	0.31	4.5
250	125	Glass	0.37	2.7	6.9
500	125	Glass	0.42	2.4	7.1
250	125	Melt	2.4	0.42	6.9
250	150	Glass	1.7	0.59	5.6

In principle, the Avrami model can only be used until impingement of the growing crystals occurs. This is especially important if one wishes to use the Avrami exponent to discuss the type of crystal growth (e.g., 1-dimensional or needle-like). In this case, the Avrami model is used only to fit the experimental sigmoidal curves and to estimate the time at half crystallization ($t(\chi = 0.5)$ or $t_{½}$). The reciprocal value of $t_{½}$ can be taken as a measure of the crystallization rate. The time at half crystallization of the sample crystallized at 70 °C from the glassy state is 3.3 min, whereas the one annealed at 125 °C from the glassy state is 0.37 min and the one at 125 °C from melt state is 2.4 min. Before discussing the crystallization rate in more detail, it should be mentioned that the crystallization isotherms for annealing at 125 °C after heating from the glassy state obtained using faster (500 K min^{-1}) or slower heating (250 K min^{-1}) rates are very comparable, indicating that these heating rates are sufficiently fast not to affect the results.

The crystallization during the isothermal annealing of the blend from the glassy state is faster when the blend is crystallized (annealed) at 125 °C as compared to 70 or 150 °C (the subsequent heating was at 250 K min^{-1} in each case). This is in agreement with the universal behavior of the crystallization rate, showing a maximum rate between T_g and T_m [20]. Closer to T_m it decreases due to the reduction of the undercooling (the difference between the thermodynamic melting point and the crystallization temperature; this is the thermodynamic driving force for crystallization). Closer to T_g it decreases due to the reduction of the (cooperative) mobility.

Last but not least, one observes that the crystallization process at 125 °C occurs faster during annealing from the glassy state than from the melt state. Although crystallization is avoided during rapid cooling, quenching below the T_g and subsequently heating to the isothermal annealing temperature still increases the number of active nuclei, as compared to the number of nuclei formed during cooling (at similar rates) from the melt to the isothermal crystallization temperature. The additional active nuclei will

contribute to the nucleation mechanism at the T_{iso-x} during isothermal annealing and will thus result in a faster crystallization (at the same temperature) for samples annealed from the glassy state as compared to samples annealed at from the melt state [21, 22].

Conclusions

RHC permits one to analyze the kinetics of fast crystallization processes, down to crystallization times of a few seconds. In this article, the isothermal annealing of P3HT:PCBM (1:1) polymer-fullerene blends for bulk heterojunction solar cell was studied using RHC. The kinetics of crystallization processes taking less than 2 min and involving at most 8 J g^{-1} could be followed quantitatively. The results indicate a higher crystallization rate around 125 °C and slower crystallization rates at 70 and 150 °C. These results are important for selecting the annealing conditions, as crystallinity improves charge conduction and cell efficiency, while overgrowth of the crystals decreases the efficiency of the solar cells. The crystallization kinetics are also thought to play an important role in the long-term thermal stability of the blend morphology developed during annealing, but further investigation in this respect is still needed.

Acknowledgements The authors acknowledge the support by the Research Foundation-Flanders (FWO-Vlaanderen) and TA Instruments.

References

1. Al-Ibrahim M, Ambacher O, Sensfuss S, Gobsch G. Effects of solvent and annealing on the improved performance of solar cells based on poly(3-hexylthiophene): Fullerene. Appl Phys Lett. 2005;86:201120.
2. Li G, Shrotriya V, Yao Y, Yang Y. Investigation of annealing effects and film thickness dependence of polymer solar cells based on poly(3-hexylthiophene). J Appl Phys. 2005;98(4):043704.
3. Yang XN, Loos J, Veenstra SC, Verhees WJH, Wienk MM, Kroon JM, Michels MAJ, Janssen RAJ. Nanoscale morphology of high-performance polymer solar cells. Nano Letters. 2005;5(4):579–83.
4. Erb T, Zhokhavets U, Gobsch G, Raleva S, Stuhn B, Schilinsky P, Waldauf C, Brabec CJ. Correlation between structural and optical properties of composite polymer/fullerene films for organic solar cells. Adv Funct Mater. 2005;15(7):1193–6.
5. Padinger F, Rittberger RS, Sariciftci NS. Effects of postproduction treatment on plastic solar cells. Adv Funct Mater. 2003;13(1):85–8.
6. Nguyen LH, Hoppe H, Erb T, Gunes S, Gobsch G, Sariciftci NS. Effects of annealing on the nanomorphology and performance of poly (alkylthiophene): fullerene bulk-heterojunction solar cells. Adv Funct Mater. 2007;17(7):1071–8.
7. Ma WL, Yang CY, Heeger AJ. Spatial Fourier-transform analysis of the morphology of bulk heterojunction materials used in "plastic" solar cells. Adv Mater. 2007;19(10):1387.
8. Thompson BC, Frechet JMJ. Organic photovoltaics—Polymer-fullerene composite solar cells. Angew Chem Int Ed. 2008;47(1):58–77.
9. Jo J, Kim SS, Na SI, Yu BK, Kim DY. Time-dependent morphology evolution by annealing processes on polymer: fullerene blend solar cells. Adv Funct Mater. 2009;19(6):866–74.
10. Bertho S, Janssen G, Cleij TJ, Conings B, Moons W, Gadisa A, D'Haen J, Goovaerts E, Lutsen L, Manca J, Vanderzande D. Effect of temperature on the morphological and photovoltaic stability of bulk heterojunction polymer: fullerene solar cells. Sol Energy Mater Sol Cells. 2008;92(7):753–60.
11. Gaisford S, Buanz ABM, Jethwa N. Characterisation of paracetamol form III with rapid-heating DSC. J Pharm Biomed Anal. 2010;53(3):366–70.
12. Miltner HE, Grossiord N, Lu KB, Loos J, Koning CE, Van Mele B. Isotactic polypropylene/carbon nanotube composites prepared by latex technology. Thermal analysis of carbon nanotube-induced nucleation. Macromolecules. 2008;41(15):5753–62.
13. Badrinarayanan P, Dowdy KB, Kessler MR. A comparison of crystallization behavior for melt and cold crystallized poly ((L)-Lactide) using rapid scanning rate calorimetry. Polymer. 2010;51(20):4611–8.
14. Mathot VBF. Crystallization of polymers. J Therm Anal Calorim. 2010;102(2):403–12.
15. De Santis F, Adamovsky S, Titomanlio G, Schick C. Scanning nanocalorimetry at high cooling rate of isotactic polypropylene. Macromolecules. 2006;39(7):2562–7.
16. Ray VV, Banthia AK, Schick C. Fast isothermal calorimetry of modified polypropylene clay nanocomposites. Polymer. 2007;48(8):2404–14.
17. Danley RL, Caulfield PA, Aubuchon SR. A rapid-scanning differential scanning calorimeter. Am Lab. 2008;40(1):9–11.
18. Zhao J, Swinnen A, Van Assche G, Manca J, Vanderzande D, Van Mele B. Phase diagram of P3HT/PCBM blends and its implication for the stability of morphology. J Phys Chem B. 2009;113(6):1587–91.
19. Avrami M. Kinetics of phase change II. Transformation-time relations for random distribution of Nuclei. J Chem Phys. 1940;8:212–24.
20. Elias H-G. Macromolecules 3. New York: Wiley; 2007.
21. Janeschitz-Kriegl H, Ratajski E, Wippel H. The physics of a thermal nuclei in polymer crystallization. Colloid Polym Sci. 1999;277(2–3):217–26.
22. Supaphol P, Spruiell JE. Isothermal melt and cold-crystallization kinetics and subsequent melting behavior in syndiotactic polypropylene: a differential scanning calorimetry study. Polymer. 2001;42(2):699–712.